OPTIMIZED OPERATION OF A COMBINED SOLAR AND WASTE HEAT DRIVEN HIGH TEMPERATURE HEAT PUMP FOR A FOOD INDUSTRY

Panteleimon Tzouganakis[1, 2*], Dimitrios Rakopoulos[1], Evangelos Bellos[1, 2], Angelos Skembris[1], Nikolaos Rogkas[1], Enrico Jende[3], Varshil Dalal[3]

[1] Centre for Research & Technology Hellas, Chemical Process & Energy Resource Institute, Athens, Greece
[2] Department of Mechanical Engineering, School of Engineering, University of West Attica, 250 Thivon & Petrou Ralli, 12244 Athens, Greece
[3] Institute of Low-Carbon Industrial Processes, German Aerospace Center (DLR), Cottbus, Germany

*Corresponding Author: (p.tzouganakis@certh.gr)

ABSTRACT

Heat upgrade to high-temperature levels is a significant challenge in the industry that accounts for high annual CO_2 emissions. This research aims to develop a novel concept for solar energy and waste heat exploitation to enable high-temperature heat upgrade through a heat pump. The design incorporates the use of solar thermal collectors connected with a thermal energy storage tank, with thermal oil as the storage medium. The stored heat in coalition with a waste heat recovery unit will operate a reverse air Brayton heat pump to achieve the required temperature. A Matlab algorithm has been developed to simulate the operation of the system dynamically. The analysis is conducted for a food industry located in Kreba-Neudorf, Germany where a temperature upgrade from 245ºC to 255ºC of a 20.7 kg/s mass flow rate of diathermic oil is required. The solar thermal collecting area installed is 500 m^2 with a 15 m^3 storage tank volume, while the waste heat availability is 2.6 kg/s flue gas mass flow rate at 230ºC. The plant is operational for 8 hours a day and 5 days per week for the year. The present work will calculate important metrics such as the average daily coefficient of performance (COP) and the daily heat production. Furthermore, a parametric investigation of various parameters of the system is conducted to achieve the highest efficiency, while the significance of the temperature of the thermal energy storage to the COP of the system is illustrated.

1 INTRODUCTION

In the EU-27, the industrial sector is the third-largest contributor to greenhouse gas emissions, producing 720 million tons of CO_2 equivalent annually. In 2020, industrial energy consumption totaled 9.68 EJ, representing 26.1% of the overall final energy demand. Approximately 80% of this energy is used for heat production at varying temperatures (Brodny and Tutak, 2022). High-temperature heat upgrades are essential for numerous industrial processes, including those in the printing and food and beverage industries (Uusitalo et al. 2020), with around 75% of this energy derived from fossil fuels (Badiei et al. 2020). Consequently, technological solutions that can deliver the required heat while minimizing CO_2 emissions would greatly benefit both industry and the environment.

Incorporating renewable energy sources into heat upgrade systems can improve their efficiency and facilitate the production of high-temperature process heat. Solar thermal systems, in particular, are considered a promising solution for sustainable and effective industrial heat upgrades. Additionally, the use of various heat pump technologies has been recognized as a viable approach for energy recovery and efficiency improvements. Recent advancements in this technology include more sophisticated cycle designs and increased performance and reliability of cycle components (Chua et al. 2010). As a result, high-temperature heat pumps (HTHPs) are now capable of raising low-grade heat sources to temperatures exceeding 100°C (Badiei et al. 2020).

The performance of a heat pump is heavily dependent on the working fluid used. Various fluids have been studied for this purpose, with the choice of the optimal fluid being influenced by factors such

as operating temperatures, power capacities, and the design of the components (Chua et al. 2010). Commonly used working fluids in high-temperature heat pumps include hydrocarbons (e.g., pentane and butane), fluorocarbons (e.g., R134a and R245fa), and simpler molecules like ammonia or CO_2 (Badiei et al. 2020). Over the years, the selection of fluids has evolved, driven in part by environmental concerns and the resulting restrictions on certain fluids due to their adverse environmental effects (Calm et. al 2011). Zhang et al. (2016) emphasize the need for ongoing research and development of new refrigerants, particularly for high-temperature heat pumps, given the limited availability of fluids that are both suitable for high temperatures and environmentally friendly.

The temperature range of the available heat is also a key factor. For medium-temperature applications, Organic Rankine Cycle (ORC) systems have proven effective, particularly in large-scale settings. Significant research over the past decade has focused on adapting ORC systems for medium and small-scale applications. However, for high-temperature waste heat sources, ORC technology is less attractive due to the lower chemical stability and higher flammability of the working fluids. In contrast, thermodynamic cycles using supercritical carbon dioxide (sCO_2) are emerging as a promising alternative for exploiting high-temperature waste heat (Marchionni et al. 2018). The advantage of sCO_2 technology lies in the unique properties of CO_2 in its supercritical state, particularly near its critical point. The cycle typically follows a Joule-Brayton configuration (Wright et al. 2009). This technology is especially appealing in applications where heat is provided at temperatures exceeding 400°C (Marchionni et al. 2018).

Despite substantial research into high-temperature heat pumps, little attention has been given to heat pumps that use a Brayton cycle with air as the working medium and waste or solar heat input as the heat source. Air, being environmentally neutral and easy to handle, offers a significant advantage. Moreover, industrial compressors can achieve temperatures greater than 200°C, with the potential to reach up to 400°C. Therefore, integrating a Brayton cycle with air as the working medium in a high-temperature heat pump for waste/solar heat utilization could offer substantial benefits for both industry and the environment.

The aim of this work focuses on exploiting solar energy to meet industrial energy needs. It explores upgrading solar heat production and waste heat recovery to generate industrial process heat at high temperatures. Previous research has been recently conducted by the authors (Tzouganakis et al. 2025) where only a solar-fed system was considered. However, in the present research, both solar and waste heat recovery are studied, and the suggested system is a highly efficient one. Specifically, the waste heat recovery unit that exploits the flue gases from the boiler will increase the efficiency of the system. The work focuses on developing a numerical model of each component, for the calculation of the dynamical response of the system during the summer period. The study examines the impact of factors such as the total collector area, the ratio of the collector area to the thermal storage tank volume, as well as the waste heat recovery unit influence on the COP of the system.

2 Materials and Methods

Figure 1 shows the studied system, which integrates solar thermal (ST) collectors coupled with a thermal energy storage (TES) tank that uses diathermic oil as a storage medium. A heat exchanger is used to facilitate the heat transfer from the pressurized water in the ST collectors to the diathermic oil in the TES tank. The reason for selecting diathermic oil in the TES tank is to avoid the requirement of a pressurized vessel in the facility. The oil stored in the TES tank is further heated from a waste heat recovery (WH) unit that is installed to exploit the high-temperature flue gases from the boiler. The oil then supplies heat to an HTHP operating on a reverse air Brayton cycle. This design is part of the SOLINDARITY project under the EU Horizon program, aimed at efficiently upgrading heat in various industrial sectors. More specifically, one of the demonstration sites of the project is the Lorenz Bahlsen Snack-World GmbH & Co KG, located in Kreba Neudorf, Germany. For this specific case, a constant diathermic oil flow rate of 20.7 kg/s is required to be upgraded from 245ºC to 255ºC on an 8/5 basis. Furthermore, the ST collectors are high vacuum flat panels which is a non-concentrated ST technology, manufactured by TVP Solar SA which is a technology provider of the SOLINDARITY project.

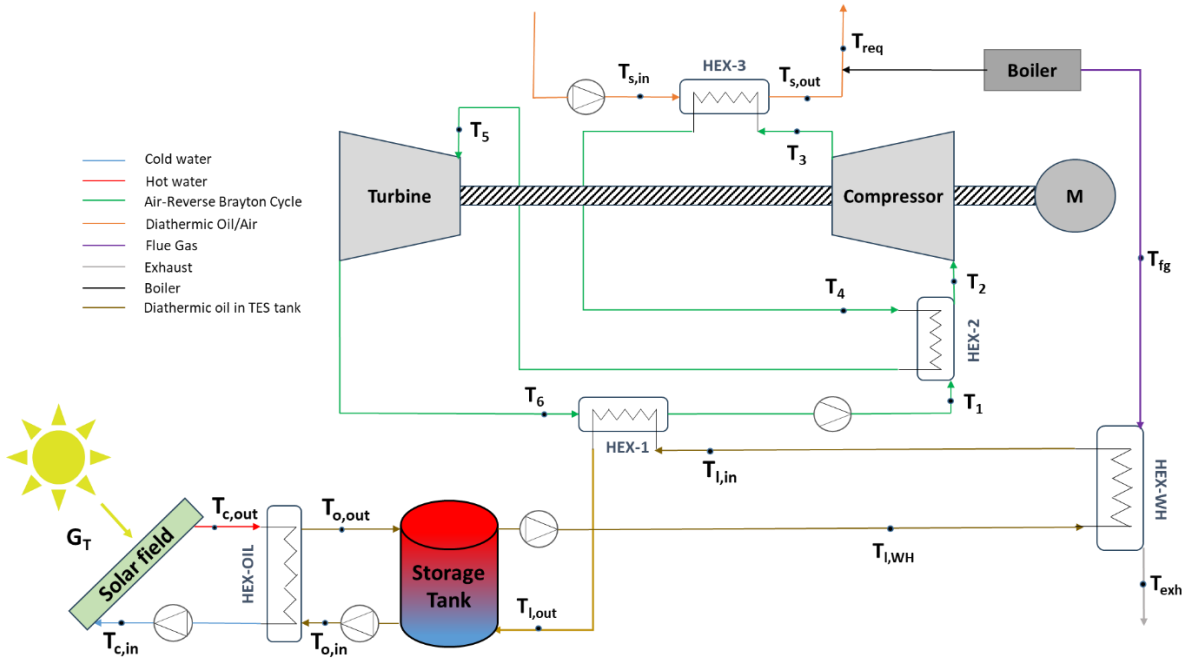


Figure 1: HTHP cycle configuration including solar thermal system, storage tank, waste heat recovery and heat pump

The HTHP operates using a reverse Brayton cycle and consists of three heat exchangers (HEX), a compressor, and a turbine, with air serving as the working medium, as shown in Figure 1. The goal of the cycle is to increase the temperature of the air in HEX-3. To achieve this, the diathermic oil heats the air in HEX-1. A recuperator (HEX-2) is used to further increase the temperature of the air in the cycle before it enters the compressor. After passing through HEX-3, the air flows through the turbine to generate power and returns to HEX-1. The compressor and turbine are connected by a shaft, which is electrically driven.

2.1 Solar Field

The solar energy is calculated by taking into account the weather data for the region of Kreba Neudorf, Germany from PVGIS. The solar energy is calculated from the Equation (1):

$$Q_{sol} = A_c \cdot G_T \tag{1}$$

where (Q_{sol}) is the solar energy, (A_c) is the total collecting area and (G_T) is the global solar irradiation. For the calculation of the global solar irradiation, parameters such as the direct normal and diffused irradiation (from weather data from the PVGIS database) and the longitude and latitude are taken into account. For the calculation of the useful heat the efficiency of the solar collectors is considered (Fischer et al. 2004):

$$\frac{Q_u}{A_c} = n_{0,b} \cdot K_\theta(\theta) \cdot G_T - c_1\left(T_{c,in} - T_{amb}\right) - c_2\left(T_{c,in} - T_{amb}\right)^2 \tag{2}$$

where (T_{amb}) and ($T_{c,in}$) are the ambient temperature and water inlet temperature in the ST collectors, while (K_θ), ($n_{0,b}$), (c_1) and (c_2) are the incident angle modifier, the zero, linear and quadratic loss coefficients of the ST collectors respectively and are obtained from the manufacturer.

The useful heat (Q_u) is transferred to water circulating the ST collectors leading to an increase in its temperature that can be calculated as:

$$Q_u = \dot{m}_c \cdot C_{p,w} \cdot (T_{c,out} - T_{c,in}) \tag{3}$$

where ($\dot{m}_c$) is the total water mass flow rate of the ST collectors, ($C_{p,w}$) is the specific heat capacity of water, while ($T_{c,out}$) is the outlet temperature of the water from the ST field.

2.2 ST-TES tank diathermic oil HEX

Due to the high temperatures that the water can reach during high global solar irradiation values, the ST collectors piping system will be pressurized to be within the saturation point. However, it is deemed beneficial in terms of safety and construction cost, to use diathermic oil as the storage medium in the TES tank, Therefore a water/diathermic oil heat exchanger will be used (HEX-OIL) as depicted in Figure 1. The modelling of the heat exchanger is obtained by considering the energy equilibriums as shown in Equations (4)-(7):

$$Q_{HEX-OIL} = \dot{m}_c \cdot C_{p,w} \cdot (T_{c,out} - T_{c,in}) \quad (4)$$

$$Q_{HEX-OIL} = \dot{m}_o \cdot C_{p,o} \cdot (T_{o,out} - T_{o,in}) \quad (5)$$

$$Q_{HEX-OIL} = UA_{HEX-OIL} \cdot \Delta T_{lm,HEX-OIL} \quad (6)$$

where ($\dot{m}_o$) is the mass flow rate of diathermic oil from the TES tank to HEX-OIL, ($C_{p,o}$) is the specific heat capacity of the diathermic oil, ($UA_{HEX-OIL}$) is the unit transfer area of the HEX-OIL, ($T_{o,in}$) and ($T_{o,out}$) is the diathermic oil temperature before and after the HEX-OIL respectively, while ($\Delta T_{lm,HEX-OIL}$) is defined as follows:

$$\Delta T_{lm,HEX-OIL} = \frac{(T_{c,out} - T_{o,out}) - (T_{c,in} - T_{o,in})}{ln\left(\frac{T_{c,out} - T_{o,out}}{T_{c,in} - T_{o,in}}\right)} \quad (7)$$

The system of Equations (4)-(7) can be solved by implementing the standard NTU method (Lienhard 2005). It should be noted that the temperature of the water after the HEX-OIL ($T_{c,in}$) will be different from the temperature used in Equation (3) to calculate the temperature increase of water due to the useful heat from the ST collectors. The temperature ($T_{c,in}$) as calculated from Equations (4)-(7) will be used in Equation (3) in the next time step of the system's simulation.

2.3 Thermal Energy Storage (TES) tank

The TES tank is commonly used in the industry to store heat during the daytime. Its thermal equilibrium can be determined by considering the heat input from the ST collectors, the heat discharged from the tank to meet the required load in HEX-1, and the heat losses to the surrounding environment. The TES tank is modeled using the mixing zone approach, as outlined in similar studies (Bellos et al. 2017). In this model, the tank is divided into N thermal zones, with each zone having a uniform temperature. Zone-1, the first zone, has the highest temperature, while Zone-N, the last zone, has the lowest. The initial temperature of the TES is (T_0) and is assumed to be uniform throughout the tank. The thermal equilibrium conditions at Zone-1, an intermediate zone (i.e. Zone -2), and Zone-N lead to the following relationships:

$$\frac{\rho_o V_t}{N} C_{p,o} \frac{\partial T_{st,1}}{\partial t} = f_1 \dot{m}_o C_{p,o}(T_{o,out} - T_{st,1}) + f_2 \dot{m}_l C_{p,o}(T_{st,2} - T_{st,1}) + \frac{U_t A_t}{N}(T_{amb} - T_{st,1}) \quad (8)$$

$$\frac{\rho_o V_t}{N} C_{p,o} \frac{\partial T_{st,2}}{\partial t} = f_1 \dot{m}_o C_{p,o}(T_{st,1} - T_{st,2}) + f_2 \dot{m}_l C_{p,o}(T_{st,3} - T_{st,2}) + \frac{U_t A_t}{N}(T_{amb} - T_{st,2}) \quad (9)$$

$$\frac{\rho_o V_t}{N} C_{p,o} \frac{\partial T_{st,N}}{\partial t} = f_1 \dot{m}_o C_{p,o}(T_{st,N-1} - T_{st,N}) + f_2 \dot{m}_l C_{p,o}(T_{l,out} - T_{st,N}) + \frac{U_t A_t}{N}(T_{amb} - T_{st,N}) \quad (10)$$

where (ρ_o) is the density of diathermic oil in the TES, (V_t) is the tank volume, (U_t) is the heat loss coefficient of the tank, (A_t) is the surface area of the tank, ($\dot{m}_l$) is the mass flow rate from the TES tank to the HTHP, ($T_{l,out}$) is the diathermic oil temperature that returns to the TES tank from the HTHP, while ($T_{st,i}$) is the temperature of the i^{th} thermal zone. Finally, (f_1) and (f_2) are parameters that regulate the mass flow in the ST-TES and TES-HTHP loop respectively depending on the system control.

2.4 Waste Heat Recovery (WHR) unit

As depicted in Figure 1 the diathermic oil from the TES tank is further heated from a WH recovery unit. The WH unit exploits the high-temperature flue gases from the boiler to increase the temperature of the diathermic oil before entering HEX-1. The modelling of the WH heat exchanger is derived by taking into account the energy equilibriums as shown in Equations (11)-(13):

$$Q_{HEX-WH} = \dot{m}_l \cdot C_{p,o} \cdot (T_{l,in} - T_{l,,wh}) \quad (11)$$

$$Q_{HEX-WH} = \dot{m}_{fg} \cdot C_{p,fg} \cdot (T_{fg} - T_{exh}) \quad (12)$$

$$Q_{HEX-WH} = UA_{HEX-WH} \cdot \Delta T_{lm,HEX-WH} \quad (13)$$

where ($\dot{m}_{fg}$) is the mass flow rate of the flue gases, ($C_{p,fg}$) is the specific heat capacity of the flue gases, (UA_{HEX-WH}) is the unit transfer area of the HEX-WH, ($T_{l,,wh}$) is the diathermic oil temperature from the TES tank before entering the WH recovery unit, (T_{fg}) and (T_{exh}) are the temperature of the flue gases and the exhaust respectively and ($\Delta T_{lm,HEX-WH}$) is defined as follows:

$$\Delta T_{lm,HEX-WH} = \frac{(T_{fg} - T_{l,in}) - (T_{exh} - T_{l,,wh})}{ln\left(\frac{T_{fg} - T_{l,in}}{T_{exh} - T_{l,,wh}}\right)} \quad (14)$$

The system of Equations (11)-(14) can be solved by implementing the standard NTU method (Lienhard 2005) like the case of the HEX-OIL.

2.5 High-temperature Heat pump

Finally, for the modelling of the HTHP, the energy equilibriums and isentropic processes have been considered for the HEXs and the compressor and turbine respectively. The HEXs in the HTHP can be modelled following the same methodology as described for the HEX-OIL and the WH recovery unit. For instance, HEX-3 can be modelled from Equations (15)-(18):

$$Q_{HEX-3} = \dot{m}_s \cdot C_{p,s} \cdot (T_{s,out} - T_{s,in}) \quad (15)$$

$$Q_{HEX-3} = \dot{m}_a \cdot C_{p,a} \cdot (T_3 - T_4) \quad (16)$$

$$Q_{HEX-3} = UA_{HEX-3} \cdot \Delta T_{lm,HEX-3} \quad (17)$$

where ($\dot{m}_s$) is the mass flow from the industrial process that requires heat upgrade, ($C_{p,s}$) is the specific heat capacity of that mass, ($\dot{m}_a$) is the mass flow of air in the reverse Brayton cycle, ($C_{p,a}$) is the specific heat capacity of air, ($T_{s,in}$) and ($T_{s,out}$) are the inlet and outlet temperatures of the industrial mass flow respectively, (T_3) and (T_4) are the air temperature before and after HEX-3, (UA_{HEX-3}) is the unit transfer area of HEX-3 and ($\Delta T_{lm,HEX-3}$) is defined as follows:

$$\Delta T_{lm,HEX-3} = \frac{(T_3 - T_{s,out}) - (T_4 - T_{s,in})}{ln\left(\frac{T_3 - T_{s,out}}{T_4 - T_{s,in}}\right)} \quad (18)$$

A similar set of Equations is derived from HEX-1 and HEX-2. The compressor will increase the pressure of air in the cycle and as a consequence the temperature to meet the requirements in HEX-3. The power required in the compressor can be calculated from Equation (19):

$$P_{com} = \dot{m}_a \cdot (h_3 - h_2) \quad (19)$$

where (h_2) and (h_3) are the enthalpies before and after the compressor and (P_{com}) the power in the compressor. For the calculation of specific enthalpies, the isentropic efficiency of the compressor will

be used, taking into account the compressor map provided by the manufacturer as a function of the air mass flow rate and pressure ratio.

The power generated in the turbine can be calculated from Equation (20):

$$P_{tur} = \dot{m}_a \cdot (h_5 - h_6) \tag{20}$$

where (h_5) and (h_6) are the enthalpies before and after the turbine and (P_{tur}) the power in the turbine. For the calculation of the specific enthalpies the isentropic efficiency of the turbine will be used, taking into account the turbine map provided by the manufacturer as a function of the air mass flow rate and pressure ratio.

The electric power required to drive the compressor-turbine shaft can be calculated from Equation (21):

$$P_{el} = \frac{1}{n_{mot}} \left(\frac{P_{com}}{n_{m,com}} - n_{m,tur} \cdot P_{tur} \right) \tag{21}$$

where (n_{mot}), ($n_{m,com}$) and ($n_{m,tur}$) are the mechanical efficiencies of the motor, the compressor and the turbine respectively, while (P_{el}) is the electric power.

From the system of Equations of the HTHP, the air temperatures of the cycle and the required mass flow rates to achieve the required temperature increase in HEX-3 can be calculated. It should be noted that the system of Equations is non-linear and therefore an iterative method is required for its solution.

As a consequence, the coefficient of performance (COP) can be determined from Equation (22):

$$COP = \frac{Q_{HEX-3}}{P_{el}} \tag{22}$$

2.6 System Control

In Equations (8)-(10) two control parameters, (f_1) and (f_2) are introduced and are used to control the ST-TES and TES-HTHP loop respectively in order to achieve optimal performance. Their control is based on the following:

- The ST-TES loop is activated when solar irradiation exceeds 100 W/m^2 to prevent operation under low irradiation conditions. When irradiation is above the specified threshold, $f_1 = 1$, whereas $f_1 = 0$ when irradiation falls below this limit.
- The TES-HTHP loop operates when the temperature of the diathermic oil is higher than 90°C at the top of the TES tank in order to achieve high COP values with the exploitation of the available waste heat. When the TES-HTHP loop operates $f_2 = 1$, while $f_2 = 0$ when the TES-HTHP loop is closed.
- The system operates on an 8/5 basis. Therefore, when the industrial process is closed the TES-HTHP loop is closed $f_2 = 0$, while the ST-TES loop parameter value depends on the irradiation profile.

2.7 Followed Methodology

In order to demonstrate the dynamical response of the proposed concept the following case study was made for a typical August week in Kreba Neudorf, Germany (6/8-11/8) that is operational from Monday to Friday between 09:00-17:00. A MATLAB algorithm was developed to simulate the dynamical response of the system. At each time step of the simulation and in accordance with the system's control, the global solar irradiation and the useful heat from the ST collectors were calculated. The transient thermal response of the TES tank was calculated taking into account the diathermic oil mass flow rates and temperatures from the HEX-OIL and the return from the HTHP. In the TES tank, a total number of 20 thermal zones have been selected. Furthermore, the time step of the simulation has been selected to 5 seconds. The initial time of operation was considered to be 00:00, while the initial TES tank

temperature was assumed to be 85°C. Finally, the EBSILON®Professional software was used for the simulation of the HTHP to facilitate the incorporation of the compressor/turbine maps, as well as pressure drops in the heat exchangers and in the piping system according to similar studies in the literature (Jende et al. 2023). The HTHP system of Equations was solved for different inlet temperatures of diathermic oil in HEX-1, to represent different operational conditions. The EBSILON®Professional software calculated the required air mass flow rate and pressure ratio to meet the required output in HEX-3. As a result, a dynamical simulation was performed that included all the components interactions, to obtain important results on the system's performance. The parameters used in the selected case study are presented in Table 1.

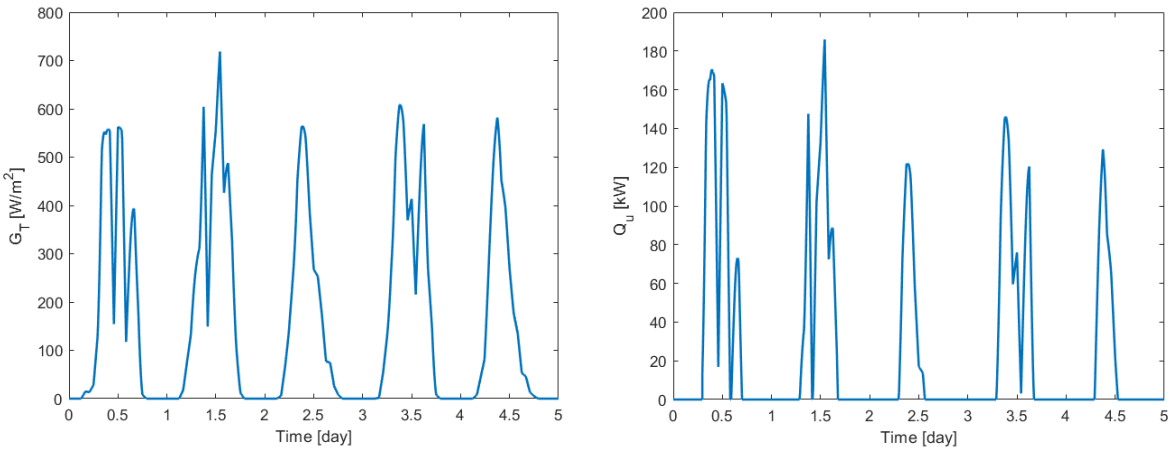
Table 1: Simulation Input Parameters

Parameter	Unit	Value
A_c	[m^2]	500
$\dot{m}_c$	[kg/s]	10
$\dot{m}_{fg}$	[kg/s]	2.6
$\dot{m}_s$	[kg/s]	20.7
T_{fg}	[°C]	230
$T_{s,in}$	[°C]	245
$T_{s,out}$	[°C]	255
UA_{HEX-1}	[W/K]	15400
UA_{HEX-2}	[W/K]	21200
UA_{HEX-3}	[W/K]	16300
UA_{HEX-WH}	[W/K]	3000
U_T	[$W/m^2/K$]	0.5
V_t	[m^3]	15

3 RESULTS & DISCUSSION

3.1 Analysis of Basic Scenario

Figure 2 depicts the expected global solar irradiation for Kreba Neudorf, Germany (6/8-11/8) as calculated from data obtained from PVGIS and the useful heat from the ST collectors (b) with respect to time.



(a) (b)

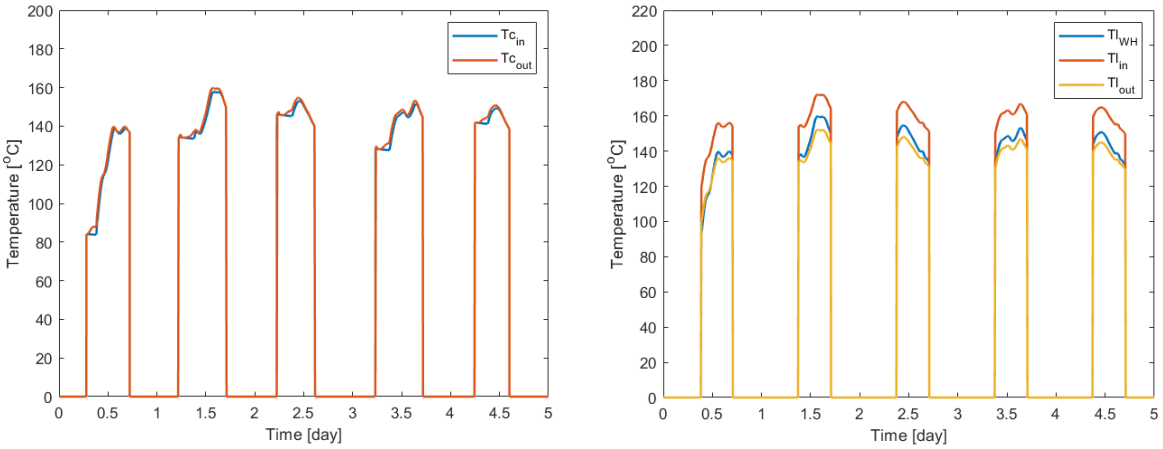
Figure 2: (a) Global solar irradiation and (b) Useful Heat with respect to time

From Figure 2(a) it is shown that the maximum global solar irradiation could reach 700 W/m^2 during noon hours. However, the irradiation profiles appear to be fluctuating which is attributed to bad weather conditions during the selected week of simulation. The maximum useful heat from the ST collectors that is transferred to the HEX-OIL is 180 kW as demonstrated in Figure 2(b). In Table 2, the HTHP results for different inlet temperatures of the diathermic oil in the HEX-1 are presented, as obtained from the performed EBSILON®Professional simulations similar to the case presented in (Jende et al. 2023).

Table 2: HTHP results for different inlet temperatures in HEX-1

m_l (kg/s)	$T_{l,in}$ (°C)	Pressure ratio	m_a (kg/s)	P_{com} (kW)	P_{tur} (kW)	COP
3.566	90	2.342	4.181	703.59	261.54	1.36
3.665	100	2.353	4.148	702.77	267.80	1.38
3.758	110	2.363	4.115	701.97	273.97	1.40
3.846	120	2.373	4.083	701.18	280.05	1.42
3.929	130	2.383	4.052	700.40	286.04	1.45
4.008	140	2.394	4.021	699.64	291.95	1.47
4.083	150	2.401	3.991	698.90	297.81	1.50
4.154	160	2.409	3.962	698.17	303.62	1.52
4.221	170	2.417	3.933	697.46	309.36	1.55

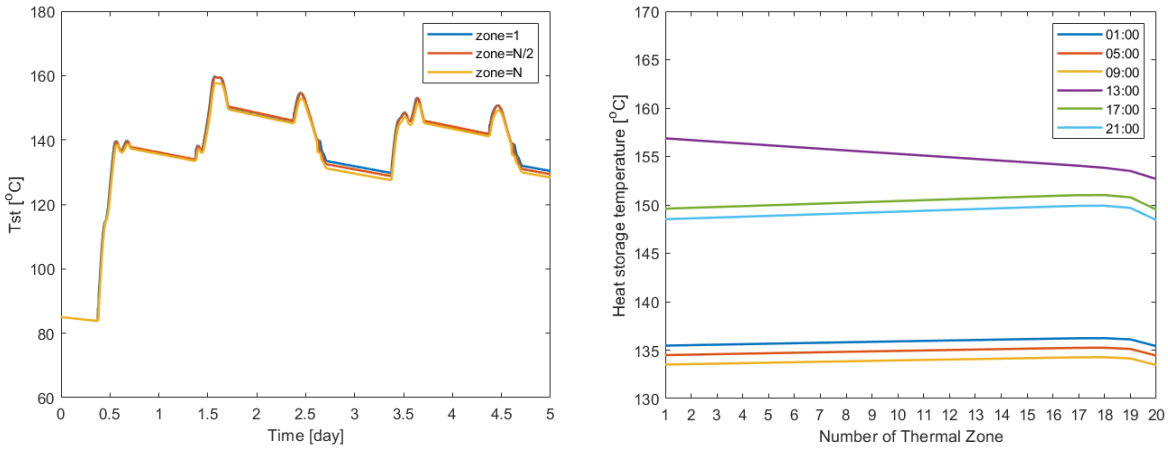
Figure 3(a) depicts the water temperature before and after the ST collectors. The temperature increment is small which is attributed to the selected water mass flow rate in the ST collectors. In Figure 3(b) the temperature of diathermic oil at various points in the system is presented. The influence of the WH unit can be observed as it increases the temperature of the diathermic oil by approximately 20°C.



(a) (b)

Figure 3: (a) Water in ST collectors and (b) diathermic oil at various points temperature with respect to time

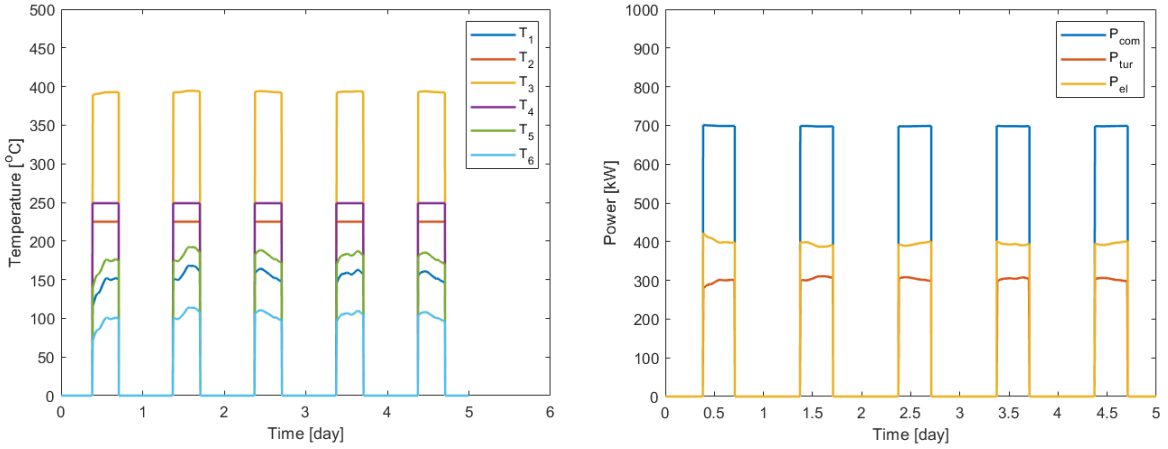
Figure 4(a) shows the temperature of the diathermic oil in the TES tank at different thermal zones with respect to time. The thermocline effect is evident during the third day of simulation. In Figure 4(b) the temperature distribution of the diathermic oil in the TES tank at different hours of the final day of the simulation is presented. The rapid temperature increase from 09:00 to 13:00 is attributed to the operation of the ST-TES loop. In addition, during the night hours the temperature drop is small, a phenomenon that is attributed to the good insulation of the TES tank.



(a) (b)

Figure 4: (a) Diathermic oil temperature at different thermal zones with respect to time and (b) thermocline at different hours during the final day

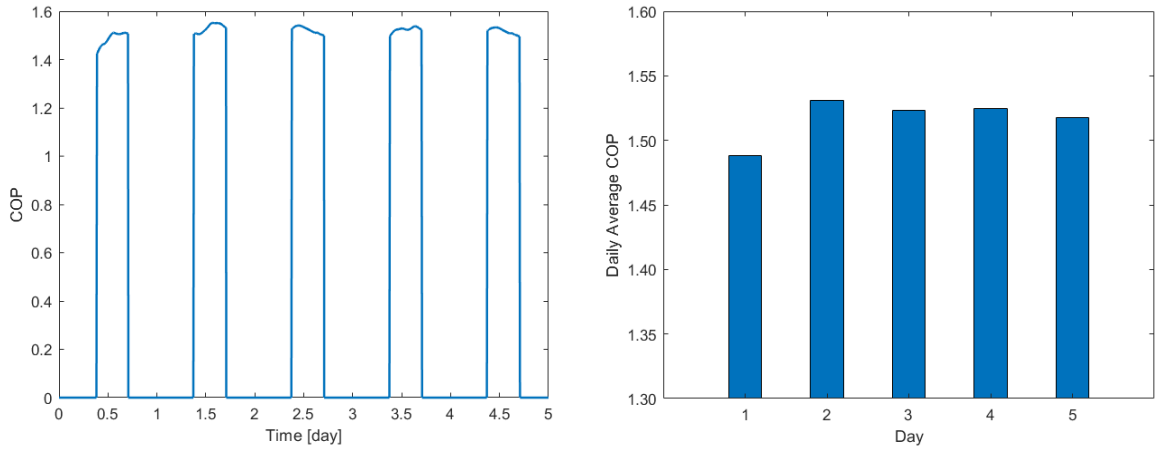
Figure 5(a) depicts the temperature of air in the reverse air Brayton cycle at six different locations according to Figure 1. The required power in the compressor, the generated power from the turbine and the electric power required to drive the compressor-turbine shaft are presented in Figure 5(b).



(a) (b)

Figure 5: (a) Air temperatures and (b) required powers in the HTHP with respect to time

From the dynamic simulation of the system, the required electric power to drive the compressor-turbine shaft is obtained and therefore the COP of the system can be calculated with respect to time. In Figure 6(a) the COP of the HTHP with respect to time is presented. It can observed that the COP fluctuates between 1.44 in the early morning to 1.56 during the noon hours. The lower values during the first day of the simulation are attributed to the initial temperature of the TES tank which was set at 85°C. In addition, the system appears to have a stable operation with minor fluctuations a phenomenon that is attributed to the thermal inertia provided by the TES tank. The HTHP is operational on the entire window of 09:00-17:00 which indicates that the system could meet the industrial requirements. In Figure 6(b) the daily average COP of the HTHP is shown. An average COP of 1.517 during summer days is expected according to the performed dynamical simulation.



(a) (b)

Figure 6: (a) COP of the HTHP with respect to time and (b) Daily average COP of the HTHP

3.2 Parametric Investigation

An important parameter in the HTHP performance is the temperature of the diathermic oil that enters HEX-1 as can be seen from Table 2. The TES tank temperature is directly linked to the total collecting area of the ST panels and their volume. Therefore, a parametric investigation of the influence of those two parameters on the COP of the HTHP is deemed necessary to achieve optimal efficiency. Figure 7 depicts the average COP of the system, for different collecting areas and ratios of the total collecting area to the TES tank volume. It is demonstrated that, as expected, the total collecting area slightly improves the COP of HTHP. In addition, the ratio of 30 m^2/m^3 yields the highest average COP.

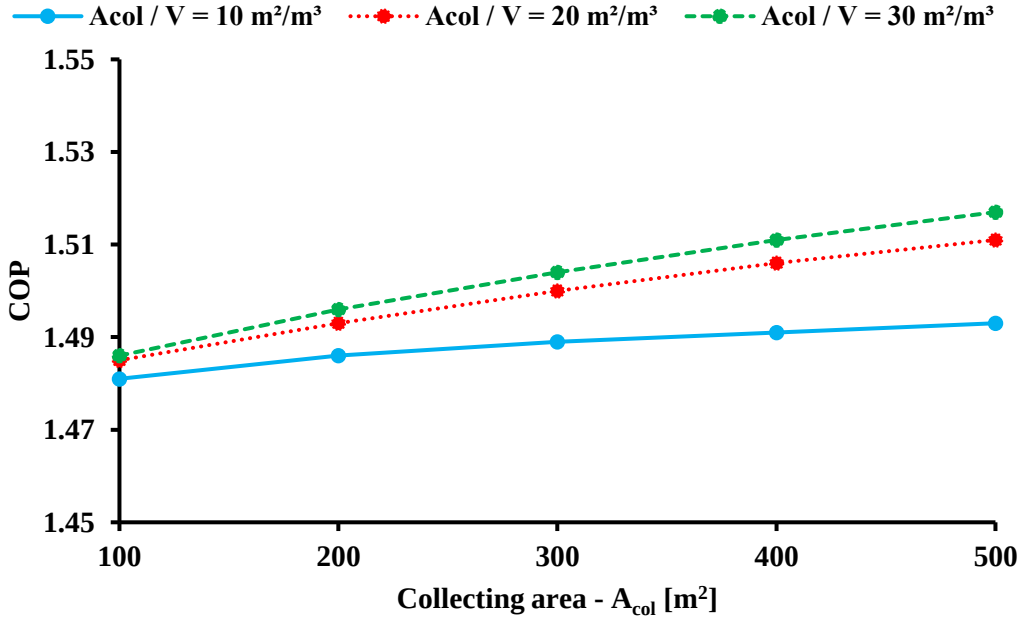


Figure 7: Average COP for different collecting areas and ratios of the TES tank

Another critical parameter that influences the diathermic oil temperature inlet in HEX-1, is the WH recovery unit. Therefore, a parametric investigation on the influence of the units of transfer area of the HEX-WH to the daily average COP of the HTHP is deemed necessary, to determine the optimal design point, that combines efficiency increment while maintaining a cost-effective design. In Figure 8 the average COP for different values of units of transfer area of HEX-WH is presented. It can be observed that the optimal design point is at 5000 W/K, where a COP value of 1.55 is approximately achieved.

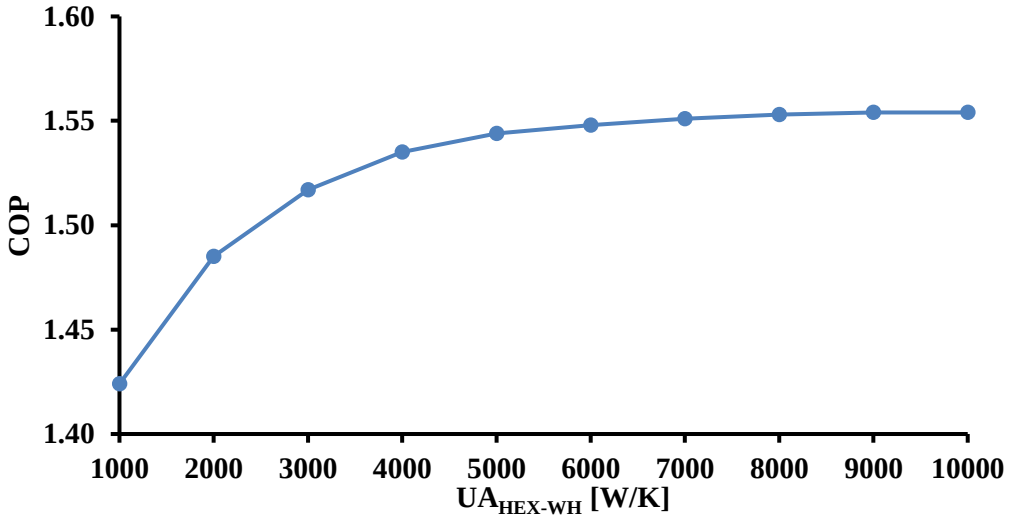


Figure 8: Average COP for different HEX-WH designs

4 CONCLUSIONS

This research proposes a system for upgrading heat to high temperatures using solar energy and waste heat recovery. It combines solar thermal collectors, thermal energy storage, waste heat recovery and a reverse air Brayton heat pump. A Matlab algorithm simulates the system's operation in a food industry in Kreba-Neudorf, Germany, where a temperature upgrade from 245°C to 255°C of a 20.7 kg/s mass flow rate of diathermic oil is required. The system includes 500 m² of solar collectors, a 15 m³ storage tank, while the waste heat availability is 2.6 kg/s flue gas mass flow rate at 230ºC. A daily average COP of 1.517 was calculated while a parametric investigation on the influence of various design parameters such as the total collecting area, the ratio of collecting area to TES tank volume and the units of transfer area of the waste heat unit was conducted to obtain the optimal design point. The future research will aim at simulating the system for longer periods, including winter operation, and integrating environmental and economic criteria to thoroughly optimize the system components. Finally, the model could be enhanced with the inclusion of heat losses in the piping of the system, while a CFD analysis could be conducted to validate the results of the thermal response in the TES tank.

NOMENCLATURE

A	Area	[m^2]	**Subscripts**	
C_p	Specific heat capacity	[J/kg/K]	a	Air
COP	Coefficient of performance	[-]	amb	Ambient
G	Solar irradiation	[W/m^2]	c	Collector
h	Specific enthalpy	[J/kg]	com	Compressor
$\dot{m}$	Mass flow rate	[kg/s]	el	Electric
P	Power	[W]	fg	Flue gases
Q	Heat rate	[W]	in	Inlet
T	Temperature	[ºC]	l	TES- HTHP loop
U	Heat loss coefficient	[$W/m^2/K$]	o	Diathermic oil
UA	Units of the transfer area	[W/K]	out	Outlet
V	Volume	[m^3]	s	Heat sink
Greek			sol	Solar
ρ	Density	[kg/m^3]	t	tank
			u	Useful
			w	Water

REFERENCES

Badiei, A., Akhlaghi, Y. G., Zhao, X., et al. (2020). *A chronological review of advances in solar assisted heat pump technology in 21st century*. Renewable and Sustainable Energy Reviews, 132, 110132.

Bellos, E., & Tzivanidis, C. (2017). *Parametric analysis and optimization of a solar driven trigeneration system based on ORC and absorption heat pump*, Journal of Cleaner Production, 161, 493-509

Brodny, J., & Tutak, M. (2022). *Analysis of the efficiency and structure of energy consumption in the industrial sector in the European Union countries between 1995 and 2019*. Science of The Total Environment, 808, 152052.

Calm, J. M., & Hourahan, G. C. (2011, August). *Physical, safety, and environmental data for current and alternative refrigerants*. In Proceedings of 23rd international congress of refrigeration (ICR2011), Prague, Czech Republic (pp. 21-26).

Chua, K. J., Chou, S. K., & Yang, W. M. (2010). *Advances in heat pump systems: A review*. Applied energy, 87(12), 3611-3624.

Fischer, S., Heidemann, W., Muller-Steinhagen, H., Perers, B., Bergquist, P. & Hellstrom, B. (2004). *Collector test method under quasi-dynamic conditions according to the European Standard EN 12975-2*, Solar Energy, 76, 117–123.

Jende, E., Kabat, N., Stathopoulos, P., & Nicke, E. (2023). Thermodynamic analysis of an industrial process integration of a reversed Brayton high-temperature heat pump: A case study of an industrial food process. In E3S Web of Conferences (Vol. 414, p. 03006). EDP Sciences.

Lienhard, J. H. (2005). A heat transfer textbook. Phlogistron.

Marchionni, M., Bianchi, G., & Tassou, S. A. (2018). *Techno-economic assessment of Joule-Brayton cycle architectures for heat to power conversion from high-grade heat sources using CO2 in the supercritical state*. Energy, 148, 1140-1152.

Tzouganakis, P., Bellos, E., Rakopoulos, D., Skembris, A., & Rogkas, N. (2025). *Thermodynamic analysis of a solar-fed heat upgrade system using the reverse air Brayton cycle*. Renewable Energy, 238, 121975.

Uusitalo, A., Turunen-Saaresti, T., Honkatukia, J., Tiainen, J., & Jaatinen-Värri, A. (2020). Numerical analysis of working fluids for large scale centrifugal compressor driven cascade heat pumps upgrading waste heat. Applied energy, 269, 115056.

Wright, S. A., Pickard, P. S., Fuller, R., Radel, R. F., & Vernon, M. E. (2009, January). Supercritical CO2 Brayton cycle power generation development program and initial test results. In ASME power conference (Vol. 43505, pp. 573-583).

Zhang, J., Zhang, H. H., He, Y. L., & Tao, W. Q. (2016). *A comprehensive review on advances and applications of industrial heat pumps based on the practices in China*. Applied Energy, 178, 800-825.

ACKNOWLEDGEMENT

This work has been supported financially by the EU Horizon, research project SOLINDARITY (Grant agreement ID: 101136148).